J. Electrochem. Sci. Eng. **8(1)** (2018) 101-110; DOI: http://dx.doi.org/10.5599/jese.476

Open Access : : ISSN 1847-9286

https://pub.iapchem.org/ojs/index.php/JESE

Original scientific paper

Influence of aging on the heat and gas emissions from commercial lithium ion cells in case of thermal failure

Michael Lammer✉, Alexander Königseder, Peter Gluschitz, Viktor Hacker

Institute of Chemical Engineering and Environmental Technology, Graz University of Technology, Inffeldgasse 25C, 8010 Graz, Austria

Corresponding authors E-mail: ✉michael.lammer@tugraz.at; Tel.: +43 316 873 8795; Fax: +43 316 873 8782

Received: November 22, 2017; Revised: December 27, 2017; Accepted: January 8, 2018

Abstract

A method for thermal ramp experiments on cylindrical 18650 Li-ion cells has been established. The method was applied on pristine cells as well as on devices aged by cyclisation or by storage at elevated temperature respectively. The tested cells comprise three types of $LiNi_{0.8}Co_{0.15}Al_{0.05}O_2$ cells for either high power or high energy applications. The heat flux to and from the cell was investigated. Degradation and exothermic breakdown released large amounts of heat and gas. The total gas and heat emission from cycled cells was significantly larger than emission from cells aged by storage. After aging, the low energy cell ICR18650HE4 did not transgress into thermal runaway. Gas composition changed mainly in the early stage of the experiment. The composition of the initial gas release changed from predominantly CO_2 towards hydrocarbons. A comparable mixture of H_2, CO and CO_2 were emitted in all tests during thermal runaway.

Keywords

Battery characterisation; thermal runaway; gas analysis; heat quantification

Introduction

Recent events like burning phone batteries, notebook computers and battery fires on planes and electric car incidents have shown the intrinsic hazard potential connected to lithium ion battery systems [1–5]. The high energy density of these devices also implies the risk of catastrophic failure in case of malfunction. Safety and risk related issues thus are not only of concern for end users, but also for producers of cells and battery packs and for transportation policy makers [6]. In Li-ion cells the two highly reactive electrodes are separated by a thin polymer separator to prevent direct contact. Ionic conductivity is achieved by an organic aprotic solvent containing the conducting salt. Electrolyte flammability further increases the volatility of this particular electrochemical system. Accumulation of heat within the cell, *i.e.* either excessive external heat influx or heat generation

surpassing the ability of dissipation, poses a serious threat to the integrity of the device [7,8]. Thermally induced degradation processes comprise the evolution of gas from evaporation and degradation of the electrolyte, melting of the separator leading to internal short circuits, changes of the electrodes' structure releasing oxygen and lithium respectively and other fast self-accelerating exothermic reactions leading to thermal runaway [9–14]. Lithium ion cells not only offer a higher energy density but also more resistance towards aging than other types of electrochemical secondary cells like Pb-acid batteries and NiMH systems [15–17]. Aging affects the overall capacity by loss of active material and decay in conductivity and reactivity. After reaching their end of usability, Li-ion cells are still reactive and potentially dangerous devices though.

Due to their importance and intrinsic risks, lithium ion cells and battery systems are subjected to rigorous testing. Most of these tests provoke thermal issues by short circuiting, heating, decay of components or combinations of these damaging effects. Widely applied mechanical testing methods involve dropping cells from defined altitudes (drop tests), crushing or piercing cells with conductive (nail tests) and non-conductive (wedge/crush tests) tools [6,18–20]. Electrical testing is performed by overcharging, deep discharging and externally short circuiting the cells [6,20–22]. Most thermal stress tests are conducted by heating the cells continuously (thermal ramp tests), step-by-step (heat-wait-seek tests) or subjecting the devices to thermal shock [6,9,10,23,24]. Investigation of thermal characteristics, especially heat flux, is typically performed using calorimetric methods like cone calorimetry or accelerated rate calorimetry (ARC) [8,24–28]. Most commonly, tests are conducted on a single cell level [29–31], but fire tests on battery packs and full size electric vehicles are also reported in the literature [32]. In these tests, cone calorimetry is usually employed to gain insight into the burning and fire evolution under air atmosphere [33]. Thermal degradation of battery components and single cells is performed using adiabatic calorimetry. The complex nature and high reactivity of lithium ion cells, especially during the fast gas release by rapid degradation reactions, raises the need for specialised equipment and specific operating procedures [33–35].

Investigations into the behaviour of aged cells under thermal stress in comparison to pristine ones are part of this work. Our group compared the heat and gas emissions of commercial cells of the cylindrical 18650 format in previous studies [9,10,36]. In this work, the tested cells comprise pristine devices as well as cells artificially fast-aged by cycling and cells aged by storing them at 60 °C. 80 % of remaining capacity was set as termination criterion for aging. This limit corresponds to the drop-out criterion for automotive application of Li-ion cells. The fully charged cells (state of charge, SoC = 100 %) are heated continuously by an external heat source in order to trigger thermally induced failure. The quantification of heat consumed and released from the device under test is performed at points of rapid temperature change. A time resolved acquisition of the venting behaviour enhanced the understanding of gas evolution. Due to the quasi-adiabatic conditions at the points of interest, reproducible data has been collected. Characteristic events like initial sudden gas release, the onset temperature of exothermic behaviour, the transgression into thermal runaway and the rapid cell deflagration have been identified. These events are subsequently used for accurate gas sampling to gain additional insight into the degradation of lithium ion cells at elevated temperature.

Experimental

A custom made test rig for thermal ramp tests on cylindrical lithium ion cells of the 18650 format was used for all of the experiments. Detailed information on the test rig has been published in RSC

Advances in 2017 [9].The test rig consists of a tube furnace equipped with a stainless steel tubular reactor for heating the cell. Inert gas (N_2) is used for purging the system and as a carrier gas stream for transporting the gaseous emissions towards the gas sampling device. Characterisation of the emission profile and gas sampling are performed by separate experiments on the same cell type. No carrier gas is used for determining the emission profile. The test rig is flushed with inert gas and left at ambient pressure. By switching to a set of communicating vessels, gas emissions directly displace fluid from the tubes. The mass of the displaced water is directly quantified by weighing and directly corresponds to the volume of released gas. A time-resolved characterisation of the gas emission is achieved by this setup.

Gas sampling is achieved by a syringe pump withdrawing a sample from the off-gas stream and transferring it into a sample vial via a multi-port valve. After the sampling operation, the valve is automatically switched and a new vial becomes available for sampling. The previously filled vial is taken to the ex-situ gas analysis by micro-GC (Agilent micro-GC 3000, USA). This method is used to collect gas samples at defined points of interest during the experiment. The first, sudden gas emission (first venting), the consecutive exothermic phase and the terminal venting after thermal runaway are considered points of interest in this work. Figure 1 shows the generic profile of a thermal ramp test.

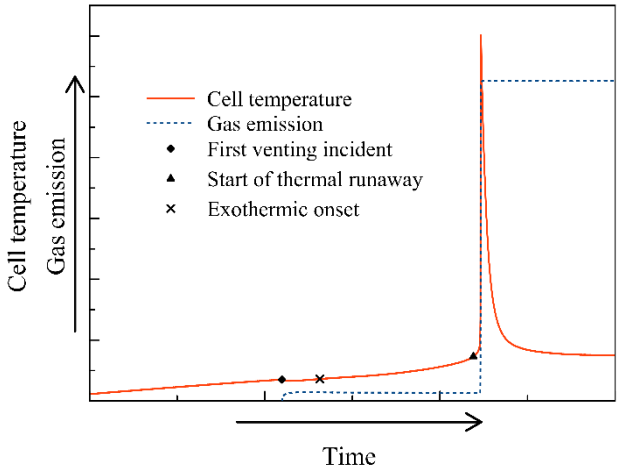

Figure 1. *Generic overview containing the characteristic events on the temperature curve and the corresponding gas emission profile*

The cells tested within this work were NCR18650BF, INR18650-35E and ICR18650HE4. All these cells consist of $LiNi_{0.8}Co_{0.15}Al_{0.05}O_2$ cathodes and graphite anodes. Although NCR18650BF and INR18650-35E are similar in regards of energy density, the cells are working quite differently, as the three types of 18650 cells show different application profiles (Table 1). Cells were used in pristine or artificially aged condition. Aging was carried out either by cyclisation or storing cells at 60 °C until a remaining capacity of 80 % was reached. The cells were cycled four times for determination of the capacity during storage. All cells were prepared by charging to 100 % of state of charge according to the manufacturer's data sheet applying a constant current/constant voltage charging routine. A BaSyTec Battery Test System (BaSyTec GmbH, Germany) was used for conditioning the cells. After charging, the plastic cover was removed, and the cell's mass was recorded. Three type-K thermocouples were fixed to the can by a sheet of glass fibre cloth. This sheet also acted as insulation material preventing short circuiting of the cell within the stainless steel sample holder. The sample holder both allowed reproducible positioning of the cell under test within the tubular reactor and leaving enough space for unhindered gas and particle emission.

Table 1. *Cells tested within the study; the application profile was established on base of the maximum discharge current and energy content calculated from manufacturer datasheets.*

Cell	Mass, g	Capacity, Ah	Energy, J	Application profile
NCR18650BF	44.87	3.35	43404	Long runtime at low power consumption
INR18650-35E	47.70	3.35	45386	High power and high energy applications
ICR18650HE4	45.50	2.50	32416	Short runtime at high power consumption

Flushing the reactor and piping with inert gas (N_2; 1 l min^{-1}, 20 min) purged the system of air. The furnace was preheated to 80 °C. Then a heating ramp of 70 W (corresponding to approx. 0.5 °C min^{-1}) was applied until the terminal venting of the thermal runaway and cell deflagration occurred. Continuous heating led to electrolyte degradation and evaporation, initiating pressure build-up within the can. To prevent uncontrolled cell rupture caused by the pressurisation of the cell by gaseous degradation products, cells of the cylindrical 18650 format are equipped with a safety rupture disk. Breaking of this disk relieved critical pressure. This event of first gas release is denominated first venting within this work. Further application of external heat influx induced a degradative condition where the cell itself became a heat source – the exothermic phase was reached. From the exothermic phase a rapid transgression into the thermal runaway was observable. As there are no specifications on thermal runaway of electrochemical devices found in literature, a self-heating rate of ≥2 °C min^{-1} had been chosen in this work to define the beginning of thermal runaway. This very fast, self-accelerating exothermic breakdown of cell components was characterised by a final release of large amounts of gas and heat, consuming the reactive components of the cell. After this deflagration event, the cell under test cooled down to reactor temperature, as indicated in Figure 1.

Basic information on a cell type was gained by a test at ambient pressure under nitrogen atmosphere with no set gas flow. Any gas release increased the pressure within the system, displacing water from the communicating tubes. This type of experiment yielded the gas emission profile as well as the thermal features of the cell, i.e. the critical temperatures of the first venting, onset of exothermic behaviour, transgression into thermal runaway and the maximum temperature during cell deflagration. Previous studies of our group have shown that the characteristic events are reproducible at the temperatures found for each type of cell [9]. Thus, the follow-up test was conducted using a nitrogen carrier gas stream of 70 cm^3 min^{-1} to transfer the gaseous degradation products from the site of emission to the sampling device. An automated syringe pump was actuated at the characteristic temperatures to withdraw a gas sample at this point. The sample was fed into sealed and argon purged vials by means of a motorised multiport valve. This method combined the timed accuracy with the reproducibility of automatized gas sampling from the vent gas stream. Once the individual vials were filled with vent gas, they were collected, and the *ex-situ* analysis was carried out on a micro-GC system set up for the quantification of H_2, CO, CO_2, CH_4, C_2H_2, C_2H_4 and C_2H_6. Designed as a two-column system, argon and helium were used as carrier gases within the gas chromatograph. This setup made argon a viable filling gas for the “empty” sample vials, as it did not interfere with the analysis.

Results and discussion

Thermal characterisation and characteristic events

The characteristic events were determined by interpretation of the cell’s (self-)heating rate. The first venting was related to the appearance of a negative heating rate, as the Joule-Thomson effect

cooled the cell. The point of inflexion in the rate vs temperature plot indicated the transgression into exothermic behaviour. A (self-)heating rate of ≥2 °C min^{-1} was defined to be the initiation of thermal runaway. An exemplary rate vs temperature plot is shown in Figure 2.

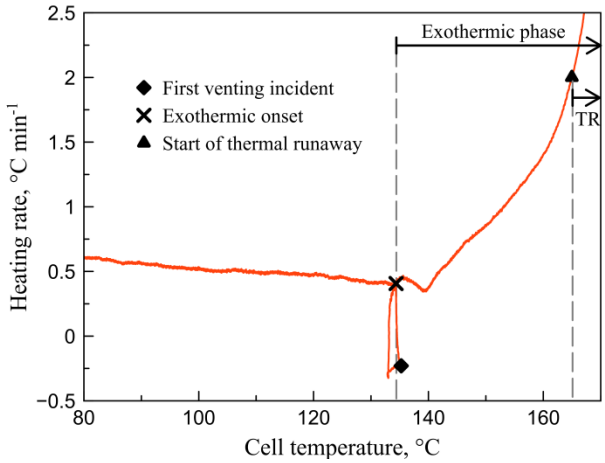

Figure 2. *Rate plot of INR18650-35E (pristine), indicating the characteristic events and the corresponding phases of exothermic behaviour and thermal runaway (TR).*

Calculation of the heat consumption and emission during the first venting incident and the thermal runaway was calculated from the temperature of the cell in relation to the thermal ramp at the respective points due to the quasi-adiabatic nature of these events. An overview of the cell temperature at the characteristic events is given in Table 2. Table 3 offers detailed information on the heat consumption and release as well as the gas emission at the respective events. Figure 3 shows the comparison of the cells under test at different states of aging. Aging effects are clearly visible in the trends of decreasing heat transfer during venting and thermal runaway respectively. The volumetric gas release does not show any clear trend. Heat calculations were performed in reproducible manner in three distinct experiments for each cell.

Table 2. *Temperature of the tested* Cells at the characteristic events*;* Status *indicates whether a cell is pristine* (a) *or aged by either cyclisation* (b) *or storage at 60 °C* (c)*;* T_{VENT} *relates to the cell temperature upon the first venting,* T_{ONSET} *is the temperature during the exothermic onset,* T_{TR} *is the temperature, at which thermal runaway was imminent and* T_{MAX} *is the maximum temperature recorded during thermal runaway.*

Cell	Status	T_{VENT} / °C	T_{ONSET} / °C	T_{TR} / °C	T_{MAX} / °C
NCR18650BF	a	134	124	172	771
INR18650-35E	a	135	115	171	695
ICR18650HE4	a	118	113	204	690
NCR18650BF	b	139	125	177	681
INR18650-35E	b	136	135	175	702
ICR18650HE4	b	116	182	203	373
NCR18650BF	c	138	119	174	618
INR18650-35E	c	136	135	172	687
ICR18650HE4	c	121	112	n.a.	n.a.

Gas release during the first venting is roughly dependent on the capacity of the cell, though the venting characteristic of NCR18650BF (new) does not fit into the scheme. The heat consumption of the first venting (Q_{VENT}) is highly consistent. Though NCR18650BF and INR18650-35E have comparable energy content, INR18650-35E consumed considerably less energy for venting. The significantly lower energy content – indicating the lowest reactivity – of ICR18650HE4 was directly

reflected by the lowest gas emission and heat consumption. The progress of the thermal runaway was consistent in regards of gas and heat release. INR18650-35E also showed lower emissions than the comparable NCR18650BF.

Table 3. *Heat and gas characteristics of the tested cells; Status indicates whether a cell is pristine (a) or aged by either cyclisation (b) or storage at 60 °C (c);* V_{VENT} *and* V_{TR} *give the amount of gas at the first venting and the thermal runaway respectively;* Q_{VENT} *and* Q_{TR} *show the relevant heat transfer;* $Q_{VENT\ REL}$ *and* $Q_{TR\ REL}$ *indicate the amounts of heat for the venting and thermal runaway relative to pristine cells;* V_{TOTAL} *gives the total gaseous emission for the duration of the test*

Cell	Status	V_{VENT} / cm³	Q_{VENT} / J	$Q_{VENT\ REL}$ / %	V_{TR} / cm³	Q_{TR} / J	$Q_{TR\ REL}$ / %	V_{TOTAL} / cm³
NCR18650BF	a	61	-212	-	5261	25541	-	5637
INR18650-35E	a	167	-136	-	5491	23682	-	5680
ICR18650HE4	a	83	-103	-	2899	21126	-	3381
NCR18650BF	b	212	-148	70	4967	22192	87	5246
INR18650-35E	b	151	-134	99	5493	17165	72	5795
ICR18650HE4	b	31	-79	77	172	7876	37	378
NCR18650BF	c	212	-135	64	5242	20624	81	5610
INR18650-35E	c	67	-78	58	5816	14482	61	5879
ICR18650HE4	c	68	-60	58	n.a.	n.a.	n.a.	69

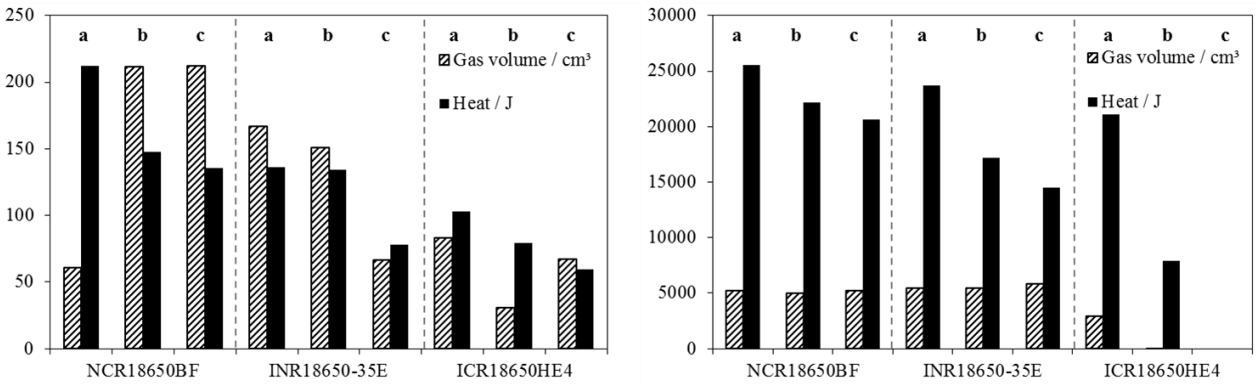

Figure 3. *Volume of released gas and heat transfer for pristine devices (a), cells aged by cyclisation (b) and cells aged by storage at 60 °C (c). The left diagram compares the first venting incident; the right diagram compares the thermal runaway. Note that heat transfer during venting is heat consumption; heat transfer during thermal runaway is heat release.*

This indicates an overall reduced reactivity of this type of cell. The low energy ICR18650HE4 degraded most severely during aging. It showed significantly lower gas and heat emissions and did not transgress into thermal runaway after aging by storage at 60 °C. Though the tested cells have the same electrode chemistry, the respective behaviour under thermal strain is different. Non-only does the electrochemically active material influence this behaviour, but also other components like the separator material and thickness, the susceptibility of the rupture disk, *etc.* Separators with higher thermal stability prevent internal short circuits until higher temperatures are reached, making the cell itself more resistant towards thermally induced failure. Venting at lower internal pressure eases the mechanical strain on the cell components. These factors have an influence on battery safety in addition to reactions within cells of similar chemical composition. In regard of reactivity loss, aging by storage at 60 °C appeared to have a more degrading effect than cyclisation. This is indicated by the lower heat consumption and emission of cells aged this way, as shown in Table 3. Total emission of gas over the duration of the experiment consisted of gas release from the

first venting after the safety rupture disk had opened, the slight gas release during the exothermic phase and the violent venting marking the terminal phase of thermal runaway. The total emission of gas is thus larger than the sum of V_{VENT} and V_{TR}.

Gas analysis at characteristic events

Gas samples were collected at the characteristic events of first venting, during the exothermic phase and after the thermal runaway. Figure 4 depicts the vent gas composition for the characteristic stages of sampling (vertical separation) and different conditions (horizontal separation).

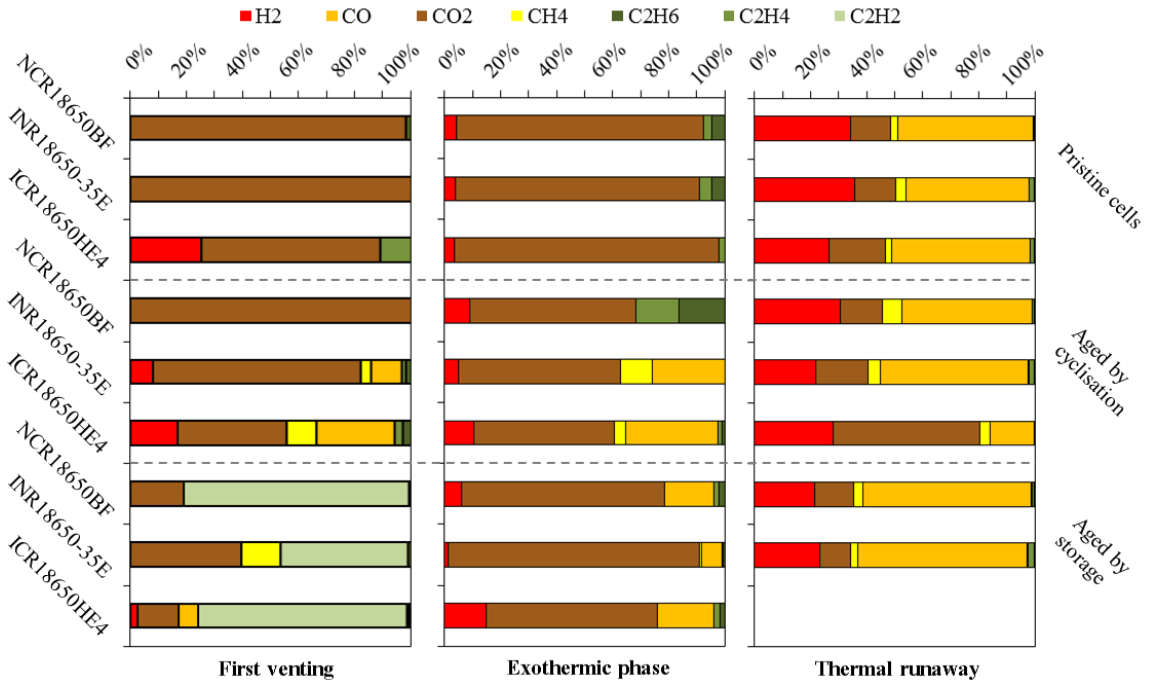

Figure 4. *Vent gas compositions at first venting, exothermic phase and thermal runaway, given for pristine specimens, cells aged by cyclisation and cells aged by storage at 60 °C. Note that ICR18650HE4 did not go into thermal runaway after aging by storage.*

Main component of the vent gas after the first release of gas was CO_2; ICR18650HE4 also released other gases like H_2, CO and CH_4 in larger concentrations than 10 %. Aging by storage drastically changed the vent gas composition at this stage, as most of the detected gas was C_2H_2 for all the cells. The exothermic phase was characterised by large quantities of CO_2. Most aged cells also emitted 10 % or more of H_2 and CO. The cycled NCR18650BF did not exhibit any CO but C_2-hydrocarbons like ethane and ethene. Gas emissions during the final stage of thermal runaway were roughly similar for all the tested cells. ICR18650HE4 showed deviations here, as the cell released larger quantities of CO_2 after aging by cyclisation and did not go into thermal runaway after aging by storage at 60 °C. This means that no gas sampling was carried out.

Gas evolution is determined by numerous factors. Decay and regeneration of the SEI layer at various states of health, reaction temperature as well as pressure within the cells influence the gas evolution and composition. Degradation of components like the organic electrolyte and consecutive gas formation within the cell during aging is not observable by the test setup, until the rupture disk gives in. A gas mixture formed during aging as well as degradation by elevated temperature is collected by the system. CO_2 is mainly deriving from decarboxylation of the organic carbonate electrolyte; CO is attributed to oxidation of carbonaceous species by oxygen released from the oxide electrode. The H_2 emission appears to be a product of the reduction of H_2O deriving from the

combustion of carbohydrates. Detailed mechanisms on the gas formation within the complex system of a Li-ion cell under thermal stress were not in the direct focus of this work and will be the aim of future investigations.

Safety considerations

In regard to safety, cells of large heat consumption during venting are considered as safer due to the possibility of cool-down below a critical level. Low emissions of heat during the thermal runaway also mark safer cells, as less heat is then spread through a battery pack or system. The evolution of gas also has to be considered, as large quantities may both exert mechanical strain on components and pose a danger due to toxic effects, fire and explosion. Large quantities of gas containing high concentrations of flammable gases, *e.g.* H_2, CO and hydrocarbons, which are in part highly toxic (*e.g.* CO), were detected in the vent gas of all cells. Thermal runaway is thus considered a highly dangerous condition also in regards of gas emission. Even cells which have reached the drop-out criterion of 80 % remaining capacity are still potentially hazardous. Safety is not determined by a universal feature – critical conditions transform devices regarded as safe into critically unsafe pieces of technology.

Conclusions

Lithium ion cells are highly susceptible to thermal stress. Inducing thermal stress by means of a tubular furnace allowed studying the associated effects in a detailed and reproducible way. Operation of the test rig under ambient pressure prevented pressure induced side reactions and created a safe and easy way to determine a gas emission profile. An estimation of the characteristic events was achieved based on these data. These events comprise the first venting, i.e. the release of gas from the previously sealed cell, the exothermic phase when the cell itself becomes a heat source and the thermal runaway. Thermal runaway of electrochemical devices is not defined in literature, thus a self-heating rate of ≥2 °C min^{-1} is used in this study. Three types of 18650 format cells were conditioned for operation – NCR18650BF, INR18650-35E and ICR18650HE4. Tests were conducted on pristine cells, devices aged by cyclisation and devices aged by storing them at 60 °C. All tests were carried out on fully charged cells.

The characteristic events were verified by investigating the (self-)heating rate of the cell. A sudden drop to negative rates was directly related to Joule-Thomson cooling initiated by gas expansion form the pressurised can. The inflexion in the heating rate signified the transgression into self-heating and thus the onset of the exothermic phase. Thermal runaway started at a self-heating rate of 2 °C min^{-1} and progressed towards total breakdown of the cell and its components, releasing large quantities of gas and heat. The heat consumed for venting and emitted in the thermal runaway had been calculated from the respective temperatures relative to the thermal ramp. Aging by storage at 60 °C showed the largest influence on the reactivity in regards of the heat and gas emissions. Cells aged this way showed the lowest emission of heat in comparison to new cells – 81 % for NCR18650BF, 61 % for INR18650-35E and no thermal runaway in case of ICR18650HE4. Gas release was only affected in the low energy cell ICR18650HE4. This device degraded the most and after aging by cyclisation it released 6 % of the volume compared to the pristine specimen. As for ICR18650HE4 aged by storage no thermal runaway was observable, no gas emission took place. We suppose that cells of similar chemistry and energy density react differently because of non-electrochemically active components like the separator setup and also because of the early venting behaviour. Thermally resistant separators shift the initiation of catastrophic internal short circuit to

higher temperature; venting releases mechanical strain on the cell components and also cools the cell. Investigation on these components is going to be conducted in the future.

Gas samples were taken at the characteristic events and analysed ex-situ. Analysis showed fairly similar behaviour for all of the cells within the same condition. Aging by storage at 60 °C led to the emission of a large proportion of C_2H_2 during the first venting. C_2H_2 is a gas observed only in traces in all other tests and situations. The evolution of C_2-hydrocarbons appears to be tightly connected to the degradation of electrolyte. The quantity of hydrocarbon emission is larger in cells aged by storage. As these cells exhibit comparable temperature at the first venting incident, it is assumed that the formation is favoured by degradation before the event, i.e. during the aging process. The main component of the vent gas during thermal runaway was CO, making the vent gas a flammable and toxic mixture. It poses a high risk of fire and explosion in regard to the high temperature associated with the event of thermal runaway.

Battery safety cannot be attributed to single features. In respect to cool-down capability during venting, heat emission during thermal runaway and gas evolution during the thermal breakdown, cells can be defined as safe. As not all types of cell show all safety criteria, e.g. a large cool-down as well as low heat emission and the release of low quantities of mainly CO_2, cells are not universally safe. Two methods for aging Li-ion cells to reach the automotive drop-out criterion of 80 % remaining capacity were applied. Aging did decrease the heat release from the cells, but still they posed a threat in case of thermally induced failure. The low capacity ICR18650HE4 cells exhibited the least reactivity after aging by storage, making them somewhat safer under these conditions. This of course comes at the price of low energy density in the first place.

***Acknowledgements**: This work and the project ISALIB is funded by the Austrian Ministry of Transport, Innovation and Technology (BMVIT) and The Austrian Research Promotion Agency (FFG) through the program "Mobilität der Zukunft" (2014-2017). Support by our research and industry partners Kompetenzzentrum - Das virtuelle Fahrzeug and Samsung SDI is gratefully acknowledged.*

References

[1] K. Bullis, *MIT Technol. Rev.* (2013). https://www.technologyreview.com/s/521976/are-electric-vehicles-a-fire-hazard/ (accessed November 15, 2017).
[2] T. V. Wilson, HowStuffWorks (2017). https://computer.howstuffworks.com/dell-battery-fire.htm (accessed November 15, 2017).
[3] A. St. John, CR Consum. Reports (2017). https://www.consumerreports.org/product-safety/whats-behind-the-increase-in-lithium-ion-battery-fires-on-planes/ (accessed November 15, 2017).
[4] A. St. John, CR Consum. Reports (2017). https://www.consumerreports.org/laptop-computers/what-to-do-if-your-laptop-catches-fire/ (accessed November 15, 2017).
[5] E. Weise, USA Today (2016). https://www.usatoday.com/story/tech/news/2016/09/02/samsung-battery-lithium-ion-fire-burning-explosion/89782856/ (accessed November 15, 2017).
[6] V. Ruiz, A. Pfrang, A. Kriston, N. Omar, P. Van den Bossche, L. Boon-Brett, *Renew. Sustain. Energy Rev.* **81** (2017) 1–26.
[7] C. Y. Jhu, Y. W. Wang, C. Y. Wen, C. M. Shu, *Appl. Energy.* **100** (2012) 127–131.
[8] Y. Fu, S. Lu, K. Li, C. Liu, X. Cheng, H. Zhang, *J. Power Sources.* **273** (2015) 216–222.
[9] M. Lammer, A. Königseder, V. Hacker, *RSC Adv.* **7** (2017) 24425-24429.
[10] A. W. Golubkov, S. Scheikl, R. Planteu, G. Voitic, H. Wiltsche, C. Stangl, G. Fauler, A. Thaler, V. Hacker, *RSC Adv.* **5** (2015) 57171–57186.
[11] P. Andersson, J. Anderson, F. Larsson, B.-E. Mellander, ESFSS 2015 2nd Eur. Symp. Fire Saf. Sci. 16 - 18 June 2015 Eur. Univ. Cyprus, Chalmers Publication Library, 2015: pp. 1–5.
[12] C. R. Birkl, M. R. Roberts, E. Mcturk, P. G. Bruce, D. A. Howey, *J. Power Sources* **341** (2016) 1–35.

[13] M. Börner, A. Friesen, M. Grützke, Y. P. Stenzel, G. Brunklaus, J. Haetge, S. Nowak, F. M. Schappacher, M. Winter, *J. Power Sources* **342** (2017) 382–392.
[14] R. Hausbrand, G. Cherkashinin, H. Ehrenberg, M. Gröting, K. Albe, C. Hess, W. Jaegermann, *Mater. Sci. Eng. B Solid-State Mater. Adv. Technol.* **192** (2015) 3–25.
[15] P. G. Balakrishnan, R. Ramesh, T. Prem Kumar, *J. Power Sources* **155** (2006) 401–414.
[16] V. Etacheri, R. Marom, R. Elazari, G. Salitra, D. Aurbach, *Energy Environ. Sci.* **4** (2011) 3243–3262.
[17] R. Zhao, S. Zhang, J. Liu, J. Gu, *J. Power Sources* **299** (2015) 557–577.
[18] D. Doughty, E.P. Roth, *Electrochem. Soc. Interface* **21(2)** (2012) 37–44.
[19] T. H. Dubaniewicz, J. P. DuCarme, *IEEE Trans. Ind. Appl.* **49** (2013) 2451–2460.
[20] R. Spotnitz, J. Franklin, *J. Power Sources* **113** (2003) 81–100.
[21] R. A. Leising, M. J. Palazzo, E. S. Takeuchi, K. J. Takeuchi, *J. Electrochem. Soc.* **148** (2001) A838.
[22] K.-H. Yen, M. Tabaddor, Y. Y. Chiang, L.-J. Chen, C. Wang, *Proceedings of the 44th Power Sources Confernce*, Las Vegas, Nevada, USA, 2010, pp. 14-18.
[23] A. Friesen, F. Horsthemke, X. Mönnighoff, G. Brunklaus, R. Krafft, M. Börner, T. Risthaus, M. Winter, F. M. Schappacher, *J. Power Sources* **334** (2016) 1–11.
[24] T. Waldmann, M. Wohlfahrt-Mehrens, *Electrochim. Acta* **230** (2017) 454–460.
[25] E. P. Roth, D. H. Doughty, D. L. Pile, *J. Power Sources* **174** (2007) 579–583.
[26] H. J. Bang, H. Joachin, H. Yang, K. Amine, J. Prakash, *J. Electrochem. Soc.* **153** (2006) A731–A737.
[27] A. Eddahech, O. Briat, J. M. Vinassa, *Energy 61* (2013) 432–439.
[28] F. Larsson, *Assessment of safety characteristics for Li-ion battery cells by abuse testing*, Thesis, Chalmers University of Technology, Göteborg, 2014.
[29] A. Hofmann, N. Uhlmann, C. Ziebert, O. Wiegand, A. Schmidt, T. Hanemann, *Appl. Therm. Eng.* **124** (2017) 539–544.
[30] E. Sarasketa-Zabala, I. Gandiaga, E. Martinez-Laserna, L. M. Rodriguez-Martinez, I. Villarreal, *J. Power Sources* **275** (2015) 573–587.
[31] Y. Troxler, B. Wu, M. Marinescu, V. Yufit, Y. Patel, A. J. Marquis, N. P. Brandon, G. J. Offer, *J. Power Sources* 247 (2014) 1018–1025.
[32] A. Lecocq, M. Bertana, B. Truchot, G. Marlair, *Proceedings from 2nd International Conference on Fires in Vehicles*, Chicago, USA, 27-28 September 2012, pp. 183-193..
[33] X. Liu, S. I. Stoliarov, M. Denlinger, A. Masias, K. Snyder, *J. Power Sources* **280** (2015) 516–525.
[34] X. Feng, M. Fang, X. He, M. Ouyang, L. Lu, H. Wang, M. Zhang, *J. Power Sources* **255** (2014) 294–301.
[35] E. Schuster, C. Ziebert, A. Melcher, M. Rohde, H. J. Seifert, *J. Power Sources* **286** (2015) 580–589.
[36] A. W. Golubkov, D. Fuchs, J. Wagner, H. Wiltsche, C. Stangl, G. Fauler, G. Voitic, A. Thaler, V. Hacker, *RSC Adv.* **4** (2014) 3633–3642.